Uzbek Journal of Physics
25(1), 46-54, 2023. DOI: https//doi.org/ 10.52304/.v25i1.405

# Structural, electronic and vibrational properties of L-asparagine

**U.A. Holikulov***

Department of Optics and Spectroscopy, Sharof Rashidov Samarkand State University, University boulevard 15, 140104, Samarkand, Uzbekistan

Received 27.01.2023, revised 15.02.2023

*Corresponding author: e-mail utkirxolikulov12@gmail.com, Phone: +99893 729 49 82

В этой работе структурные, электронные и колебательные свойства L-аспарагина были изучены с использованием спектроскопии комбинационного рассеяния и теории функционала плотности (DFT). Молекулярная геометрия цвиттер-ионного L-аспарагина (ZWASN) была оптимизирована на основе базисного набора B3LYP/6-311++G(d,p). Внутримолекулярную H-связь в цвиттер-ионном L-аспарагине анализировали с использованием методов поверхностного молекулярного электростатического потенциала (MEP), квантовой теории атомов в молекулах (QTAIM), приведенного градиента плотности (RDG), нековалентного взаимодействия (NCI) и электронных локализованных функций (ELF). Также были рассчитаны распределение атомного заряда Малликена, энергетическая щель HOMO-LUMO и другие электронные свойства. Экспериментальные спектры комбинационного рассеяния были записаны и интерпретированы с использованием методов PED.

**Ключевые слова:** L-аспарагин, цвиттер-ион, водородная связь, спектроскопия КР, метод DFT.

In this work, the structural, electronic, and vibrational properties of L-asparagine were studied using Raman spectroscopy and density functional theory (DFT) calculations. The molecular geometry of zwitterionic L-asparagine (ZWASN) was optimized based on the B3LYP/6-311++G(d,p) basis set. Intramolecular H-bonding in zwitterionic L-asparagine was analyzed using surfaces molecular electrostatic potential (MEP), quantum theory atoms in molecules (QTAIM), reduced density gradient (RDG), non-covalent interaction (NCI), and electron localized functions (ELF) methods. Mulliken atomic charge distribution, HOMO-LUMO energy gap, and other electronic properties were also calculated. Experimental Raman spectra were recorded and interpreted using PED techniques.

**Keywords:** L-asparagine, zwitterion, hydrogen bond, Raman spectroscopy, DFT method.

## I. Introduction

Amino acids are molecules that have been widely studied in recent years because they are the main components of proteins [1-6]. The presence of H-acceptor and H-donor centers such as carboxyl and amino groups in their structures is important in the secondary structure of proteins and in the process of aggregation in various solutions [3-6].

From a structural point of view, amino acids have two types of structures: neutral and zwitterionic. Basically, they are the neutral form ($H_2N$–CHR–COOH) with the most stable structure in the isolated system, that is, for the gas phase [7–10]. However, they have a zwitterionic structure ($^+H_3N$–CHR–$COO^-$) as a result of the transfer of the proton from the carboxyl group to the amino group in the crystal phase and in polar solvents [11-14].

L-asparagine ($C_4H_8N_2O_3$) is an amino acid that can be found in both protein and free form. It is also important in the metabolic modulation of cellular processes in nerve and brain tissues [15]. Because it is involved in the conversion of amino acids in the liver, it is required for the synthesis of glycoproteins and a wide range of proteins [16-20]. In Ref. [21], the conformation of asparagine was analyzed. The

DFT(B3LYP)/6-311G* and DFT(B3LYP)/6-311++G** levels of theory were used to optimize a set of 972 conformational test structures. MP2 single point energy calculations were performed on 62 stable conformations. Some H-bond displacement vibrations have also been reported to comprise realistic conformational stretching modes. Kimura [22] investigated the theoretical stability of asparagine's side-chain structure in solutions. Aleman et al. [16] theoretically examined asparagine dipeptide utilizing HF and MP2 techniques, concluding that the gauche conformation is dominant. The results of inelastic neutron scattering, infrared, Raman, and 1H NMR spectroscopy used to investigate L-asparagine dynamics are presented in the Ref. [23].

In the current work, the physical-chemical properties of the zwitterionic structure of L-asparagine were analyzed using DFT theory. We also tried to make spectral characteristics using Raman spectroscopy. Structural parameters (bond length and bond angle) and quantum chemical properties such as dipole moment, HOMO-LUMO gap, MEP surface, Mulliken charge analysis, electron affinity, ionization energy, and chemical potential were reported for the first time. Intramolecular H-bonding was analyzed using AIM, RDG, NCI and ELF.

## II. Experimental and computational details

A Renishaw Invia Raman was used to record the Raman spectra of L-asparagine in the region 400–4000 $cm^{-1}$ at room temperature. As a source of excitation light, an argon laser with a wavelength of 532 nm, a power of 50 mW, and a diffraction grating with a period of 1200 lines/mm was used. The dispersed light was recorded using a standard Renishaw CCD Camera detector.

L-asparagine geometry was optimised using the DFT approach in the Gaussian 09W programme [24]. The DFT approach, particularly with the B3LYP hybrid functional, has been successfully used to calculate molecules energies and numerous physical-chemical properties [12, 25]. In this study, we used the B3LYP functional and the 6-311++G(d,p) basis set, which includes diffusion and polarisation functionals. Furthermore, to gain a better understanding of intramolecular interactions in molecule, the topological parameters of the electron density distribution in the most stable structure were obtained using the MULTIWFN [26] tool. The results of the AIM, NCI, RDG, and ELF analyses were visualised using the tool VMD [27].

## III. Results and discussions

### III.1. Molecular geometry

The geometric structure of the zwitterionic L-asparagine was optimized based on the B3LYP/6-311++G(d,p) basis set (Fig. 1). The theoretical and experimental geometric parameters corresponding to the optimal geometry are presented in Table 1. Fig. 1 shows that there is an internal hydrogen bond (N4-H14···O1) between ionized carboxyl ($COO^-$) and amino ($NH_3^+$) groups of zwitterionic asparagine. The intermolecular hydrogen bond length is 1.8 Å.

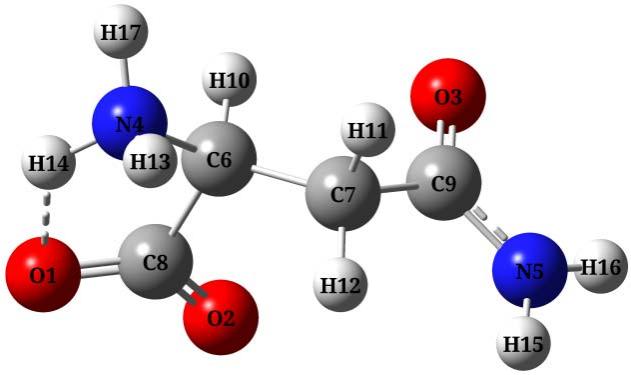



**Figure 1.** The optimal geometry of zwitterionic L-asparagine.

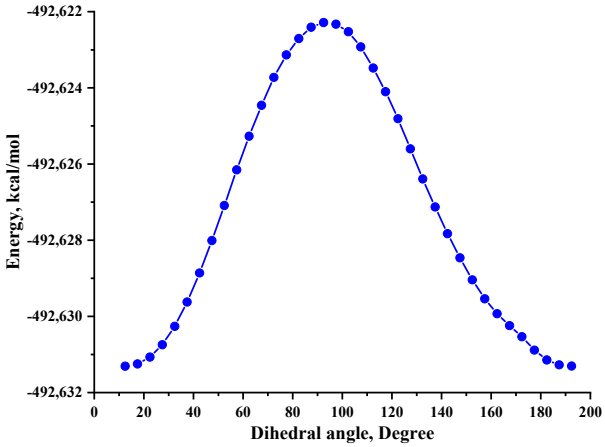



**Figure 2.** Potential energy surface scan for dihedral angle N4-C6-C8-O1 of L-asparagine.

The potential energy surface (PES) of ZWASN was scanned around the N4-C6-C8-O1 dihedral angle to localize the structure corresponding to the energy minimum (Fig. 2). The result of the scan showed that the ZWASN geometric structure with the calculated N4-C6-C8-O1 dihedral angle equal to 12.43 degrees has the minimum potential energy.

©Academy of Sciences of Republic of Uzbekistan, 2023

**Table 1.** Geometric parameters of zwitterionic L-asparagine.

| Bond length, Å | | | | | |
|---|---|---|---|---|---|
| | Calculated | Experimental [28] | | Calculated | Experimental [28] |
| H(17)-N(4) | 1.0196 | 1.00 | C(9)-C(7) | 1.5270 | 1.518 |
| H(16)-N(5) | 1.0094 | 0.94 | C(9)-O(3) | 1.2290 | 1.240 |
| H(15)-N(5) | 1.0073 | 0.92 | C(9)-N(5) | 1.3496 | 1.334 |
| H(14)-N(4) | 1.0464 | 1.01 | C(8)-O(1) | 1.2612 | 1.2407 |
| H(13)-N(4) | 1.0211 | 0.92 | C(8)-C(6) | 1.5652 | 1.536 |
| H(12)-C(7) | 1.0918 | 1.01 | C(8)-O(2) | 1.2422 | 1.262 |
| H(11)-C(7) | 1.0957 | 1.03 | C(7)-C(6) | 1.5265 | 1.535 |
| H(10)-C(6) | 1.0903 | 1.00 | C(6)-N(4) | 1.5103 | 1.485 |
| Bond angles, Degree | | | | | |
| N(5)-C(9)-O(3) | 122.8413 | 121.80 | N(4)-C(6)-H(10) | 106.7028 | 109 |
| N(5)-C(9)-C(7) | 115.5871 | 115.92 | C(7)-C(6)-C(8) | 114.6398 | 109.84 |
| O(3)-C(9)-C(7) | 121.4706 | 121.80 | C(7)-C(6)-H(10) | 109.2014 | 108.8 |
| O(2)-C(8)-C(6) | 116.0919 | 118.07 | C(8)-C(6)-H(10) | 107.9658 | 109.8 |
| O(2)-C(8)-O(1) | 129.2217 | 126.99 | C(9)-N(5)-H(15) | 122.2670 | 120.2 |
| C(6)-C(8)-O(1) | 114.6742 | 114.90 | C(9)-N(5)-H(16) | 119.3032 | 118.6 |
| C(6)-C(7)-C(9) | 111.6951 | 111.70 | H(15)-N(5)-H(16) | 118.2916 | 121 |
| C(6)-C(7)-H(11) | 109.5651 | 107.4 | C(6)-N(4)-H(13) | 113.0403 | 111 |
| C(6)-C(7)-H(12) | 110.8879 | 110.9 | C(6)-N(4)-H(14) | 102.3695 | 109 |
| C(9)-C(7)-H(11) | 105.4480 | 107.3 | C(6)-N(4)-H(17) | 113.6946 | 114.5 |
| C(9)-C(7)-H(12) | 111.4466 | 109.5 | H(13)-N(4)-H(14) | 108.2304 | 106 |
| H(11)-C(7)-H(12) | 107.5586 | 110 | H(13)-N(4)-H(17) | 108.1747 | 105 |
| N(4)-C(6)-C(7) | 112.0049 | 110.86 | H(14)-N(4)-H(17) | 111.1513 | 112 |
| N(4)-C(6)-C(8) | 105.9504 | 109.90 | | | |

It can be seen from Table 1 that the experimental and calculated results are in good agreement with each other.

### III.2. Mulliken atomic charges

Mulliken atomic charge analysis plays an important role in the use of quantum-chemical calculations to interpret the electronic structure, reactivity, dipole moment, and polarizability of a molecular system [25]. The Mulliken charge distribution for the ZWASN molecule is depicted in histogram form in Fig. 3. It can be seen from the picture that all hydrogen (H) atoms in the molecule are positively charged. Among them, H atoms bonded to nitrogen atoms are charged more than H atoms bonded to carbon atoms. The oxygen atoms in the molecule are positively charged, and the oxygens in the ionized carboxyl group (O1 and O2) have a higher electron density than the remaining oxygen (O3). Also, the nitrogen atom of the ionized amino group (N4) has a smaller electron density than the nitrogen atom of the non-ionized amino group (N5). The carbon atoms C6, C7, and C9 in the molecule are negatively charged, and the carbon atom C8 is positively charged (Fig. 2 and 3). The dipole moment of ZWASN is 13.2 Debye.

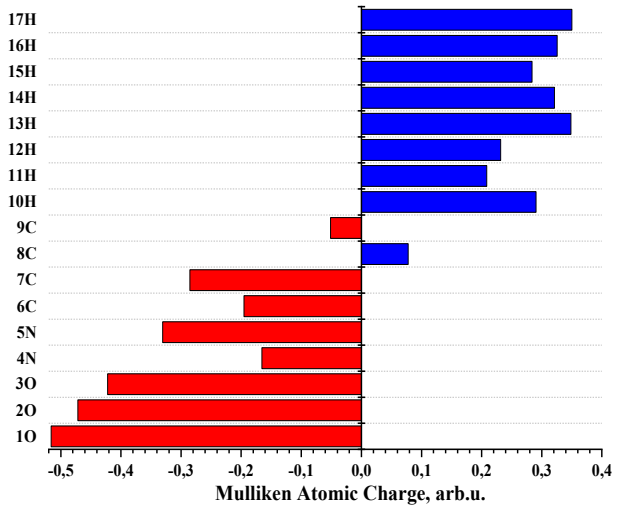



**Figure 3.** Histogram for Mulliken atomic charges of ZWASN.

©Academy of Sciences of Republic of Uzbekistan, 2023

### III.3. Molecular electrostatic potential (MEP) of surface

The molecular electrostatic potential (MEP) of surface is characterized by the electron density distribution of the atoms in the molecule. It can provide information about the physical-chemical properties of molecular systems, such as size, shape, charge density, and chemical reactivity properties. It is also used to explain electrophilic and nucleophilic reactions and to study hydrogen bonding [12]. Fig. 4 depicts the MEP surface of the zwitterionic structure of L-asparagine. Depending on the MEP level, the surfaces are represented in different colors. The colors red, yellow, green, blue are shown in increasing electrostatic potential order of the molecule. For our study, the map color code was between –0.127 (arb. units) (dark red) and 0.127 (arb. units) (dark blue) for the molecule under study, where blue color represents the region of nucleophilic reactivity (strongest attraction), and the red area indicates the region of electrophilic reactivity (strongest repulsion). The green color represents the region with zero potential. The calculated results show that negative potentials are primarily on oxygen and nitrogen atoms. Positive potentials are on the hydrogen atoms of the amino group.

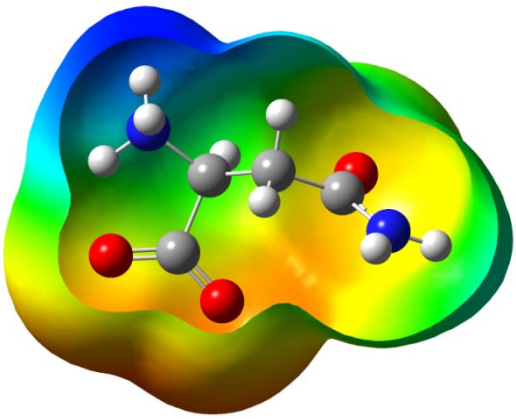


**Figure 4.** Molecular electrostatic potential (MEP) surface of ZWASN.

### III.4. Frontier molecular orbitals

The highest occupied molecular orbital (HOMO) and the lowest unoccupied molecular orbital (LUMO) are the two most important molecular orbitals that explain the chemical behavior, bioactivity, and physical properties of a molecule, and together they are called the frontier molecular orbitals. The energy difference between the HOMO and LUMO is the HOMO-LUMO energy gap. They play an important role in chemical stability. The energy gap (HOMO-LUMO) is also used to represent intramolecular charge transfer (ICT), kinetic polarization, and the electronic spectra of a molecule or system of molecules. Quantum-chemical parameters such as the global electrophilicity index, hardness, softness, electron affinity, and ionization energy can be calculated using Koopmans's theorem [29]. The frontier molecular orbitals of ZWASN are shown in Fig. 5. Using the HOMO and LUMO energies, various quantum-chemical parameters (Table 2), such as ionization energy (IE), chemical potential (μ), hardness (ε), electron affinity (EA), and global electrophilic index (ω) were calculated using the following relations:

- Hardness: $\eta = (E_{HOMO}-E_{LUMO})/2$
- Chemical potential: $\mu = (E_{HOMO}+E_{LUMO})/2$
- Global electrophilicity index: $\omega = \mu^2/2\eta$
- Ionization energy: $IE= - E_{HOMO}$
- Electron affinity: $EA= -E_{LUMO}$

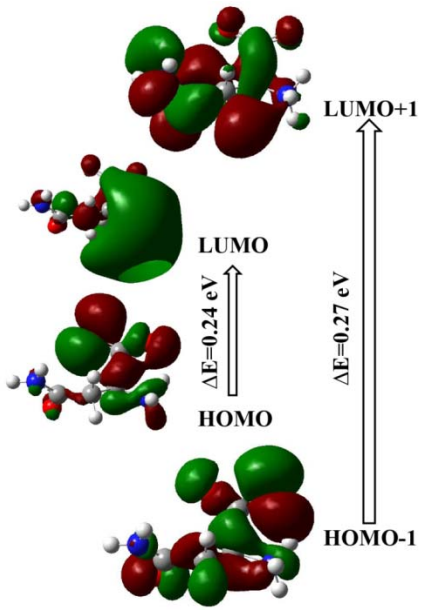



**Figure 5**. Frontier molecular orbitals diagram of ZWASN

**Table 2.** Quantum chemical parameters of ZWASN.

| | |
|---|---|
| $E_{HOMO}$ | –0.259 eV |
| $E_{LUMO}$ | –0.017 eV |
| $E_{HOMO}$-$E_{LUMO}$ | 0.242 eV |
| Hardness | 0.121 eV |
| Chemical potential | –0.185 eV |
| Global electrophilicity index | 0.007 |
| IE | 0.259 eV |
| EA | 0.017 eV |

A molecule of a large HOMO-LUMO energy gap is stable and less reactive, while a molecule of a

©Academy of Sciences of Republic of Uzbekistan, 2023

low HOMO-LUMO energy gap is reactive. The HOMO-LUMO energy gap of ZWASN is 0.24 eV, which indicates its reactivity (Table 2).

### III.5. QTAIM, RDG, NCI, and ELFanalysis

The quantum theory atoms in molecules (QTAIM) is one of the effective methods for studying intra- and intermolecular hydrogen bonds in molecular systems [12, 25]. The presence of a bond critical point (BCP) between the hydrogen atoms of the donor group and the acceptor atom, which are linked by the related bond path, is associated with the formation of hydrogen bonds. Electron density $\rho(r)$, electron density Laplacian $\nabla^2\rho(r)$ and energy density $H(r)$ at the critical points of the bond are the main topological parameters for characterizing the nature of hydrogen. Figure 6a shows the bond critical points (orange dots) in the ZWASN molecule. Electron density in BCP formed between ionized carboxyl and amino groups $\rho(r)$=0.0405 au, electron density Laplacian $\nabla^2\rho(r)$=0.1321 au. These values are in the hydrogen bond range ($\rho(r)$=0.0033–0.168 au, $\nabla^2\rho(r)$=0.020–0.139 au) [30]. The energy density has a negative value ($H(r)$=–0.005 au), and the covalent effect is dominant. This hydrogen bond energy is $E_{HB}$=10.67 kcal/mol.

Noncovalent interactions (NCI) and reduced density gradient (RDG) analyses are innovative tools for graphical visualization of weak intermolecular interactions. Quantification of the electron density of (sign λ2)ρ peaks relative to RDG provides information on the nature and strength of molecular interactions, where (sign λ2)ρ is the electron density multiplied by the sign of the second Hessian eigenvalue (λ2). In a molecular system, blue represents attractive interactions and red represents repulsive interactions; (sign λ2)ρ is critical in predicting the nature of the interaction; for example, (sign λ2)ρ<0 indicates a attractive (bonded) interaction, whereas (sign λ2)ρ>0 indicates a repulsive (unbonded) interaction. The RDG scatter plot is depicted in Fig. 6b, which shows a colored isogram of weak interactions in the ZWASN molecule. Red represents strong repulsion (steric effect), blue – hydrogen bonding interaction, and green – van der Waals interaction in Figs 6b, 6c.

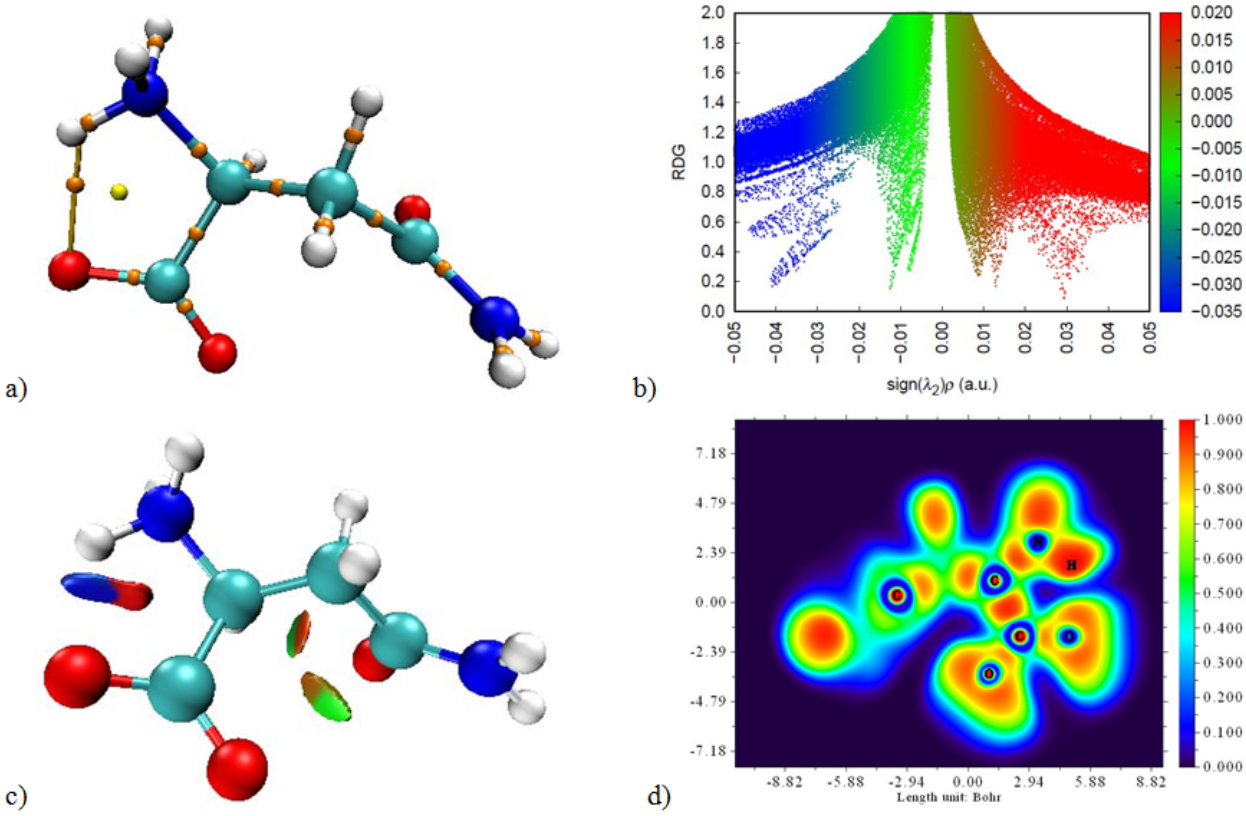



**Figure 6.** Results of QTAIM (a), NCI (b), RDG (c), and ELF (d) analysis for ZWASN.

©Academy of Sciences of Republic of Uzbekistan, 2023

Electron localization function (ELF) topological analysis is widely used to describe chemical bonds in atomic and molecular systems and to determine regions where electrons are located. ELF explains the electron pair density; the maximum number of electron pairs in the intermolecular space due to covalent bonding forms the main line of the ELF map. The ELF color map for ZWASN is shown in Fig. 6d.

If the plotted values of ELF are between 0.5 and 1.0, they have bonding and nonbonding localised electrons, however if they are less than 0.5, they have delocalized electrons. Though the interpretations are similar, the localized-orbital locator (LOL) expresses a more conclusive and flawless characterization than ELF. The red colour represents the higher end of the scale, while the blue colour represents the lower end. A delocalized electron region is indicated by a region with a value less than 0.5. Red and orange colors represent high electron localization. The region between the inner and valence shells is represented by a blue circle. The color shades of the ELF maps confirm the presence of bonding and non-bonding electrons, with the red color around hydrogen atoms having the highest value, indicating the presence of both bonding and non-bonding electrons. High ELF values around hydrogen atoms shown in red indicate high localization of electrons due to covalent bonding, a lone electron pair, or the presence of the core shell in this region. And the blue circle around the nitrogen atom shows the electron depletion region between the inner shell and the valence shell.

### III.6. Vibrational analysis

Vibrational spectra are one of the main characteristic properties of a molecule. The L-asparagine molecule consists of 17 atoms and has 45 vibrational modes. Figure 7 shows the experimental and theoretical Raman spectra of L-asparagine. Table 3 shows the results of the potential energy distribution (PED) analysis of vibration models. The VEDA programme [31] was used for PED analysis. PED analysis quantifies the fraction of vibrational energy of a group of atoms in each vibrational potential energy. The Raman bands corresponding to the N-H vibration of L-asparagine are located in the range of 3100–3600 $cm^{-1}$. The spectral peak located at 3401 $cm^{-1}$ belongs to the $NH_2$ asymmetric stretching mode. The spectral peak located at 3110 $cm^{-1}$ belongs to $NH_2$ symmetric vibrations. Spectral bands of C-H stretching located in the range of 2900–3000 $cm^{-1}$. Spectral bands of C=O stretching vibrations are located in the range of 1650–1700 $cm^{-1}$. The spectral band located at the wave number of 1694 $cm^{-1}$ belongs to the non-ionized C=O stretching vibration. The spectral peak located at 1674 $cm^{-1}$ belongs to ionized COO asymmetric stretching vibration modes. Spectral bands belonging to $NH_2$ bending vibrational modes are located in the range of 1400–1600 $cm^{-1}$.

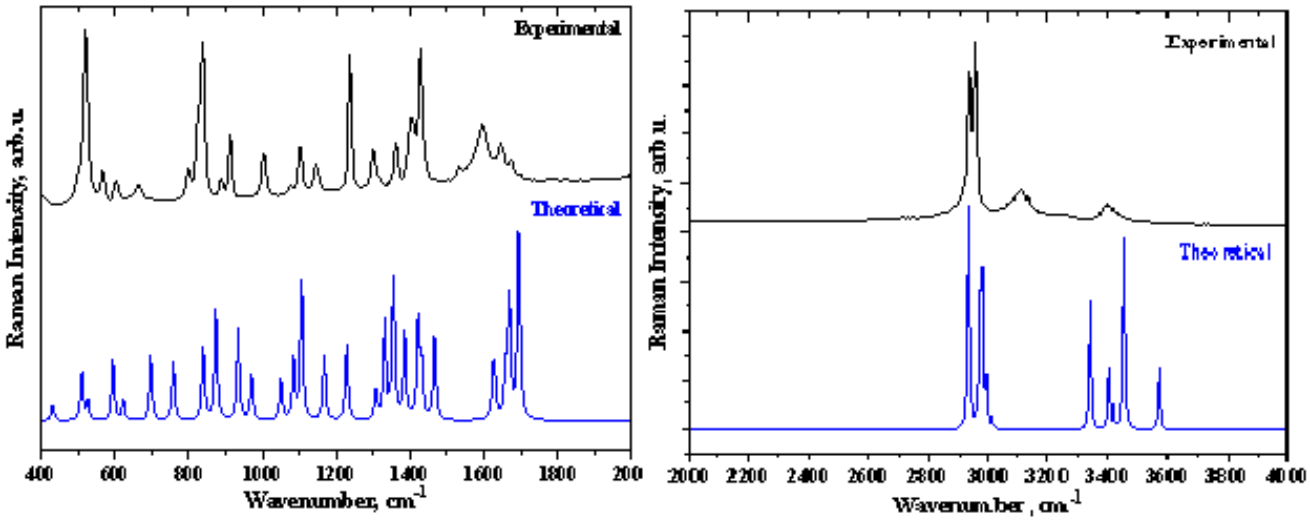



**Figure 7.** Experimental and theoretical Raman spectra of L-asparagine.

©Academy of Sciences of Republic of Uzbekistan, 2023

**Table 3.** Experimental and theoretical vibrational wavenumbers of L-asparagine

| Mode | Experimental | Calculated | Assignment (PED≥10%) |
|---|---|---|---|
| 1 | | 3575 | $\nu_{asym}(H^{15}\text{-}N^{5}\text{-}H^{16})$ 99% |
| 2 | | 3453 | $\nu_{sym}(H^{15}\text{-}N^{5}\text{-}H^{16})$ 99% |
| 3 | 3401 | 3404 | $\nu_{asym}(H^{13}\text{-}N^{4}\text{-}H^{14})$ 95% |
| 4 | 3110 | 3343 | $\nu_{sym}(H^{13}\text{-}N^{4}\text{-}H^{17})$ 95% |
| 5 | 2966 | 2999 | $\nu(C^{6}\text{-}H^{10}) + \nu(C^{7}\text{-}H^{11})$ 88% |
| 6 | 2956 | 2983 | $\nu_{asym}(H^{11}\text{-}C^{7}\text{-}H^{12})$ 83% |
| 7 | 2935 | 2975 | $\nu(N^{4}\text{-}H^{14})$ 88% |
| 8 | | 2932 | $\nu(C^{7}\text{-}H^{11})$ 87% |
| 9 | 1694 | 1694 | $\nu(C^{9}=O^{3})$ 76% |
| 10 | 1674 | 1668 | $\nu_{asym}(O^{2}=C^{8}=O^{1})$ 73% + $\delta(H^{13}\text{-}N^{4}\text{-}H^{17})$ 11% |
| 11 | 1643 | 1658 | $\delta(H^{13}\text{-}N^{4}\text{-}H^{17})$ 73% –$\tau(H^{13}\text{-}N^{4}\text{-}C^{6}\text{-}C^{7})$ 23% |
| 12 | 1596 | 1629 | $\nu_{asym}(O^{2}=C^{8}=O^{1})$ 12% –$\delta(H^{13}\text{-}N^{4}\text{-}H^{17})$ 65% |
| 13 | 1532 | 1624 | $\delta(H^{16}\text{-}N^{5}\text{-}H^{15})$ 77% – $\delta(H^{15}\text{-}N^{5}\text{-}C^{9})$ 10% |
| 14 | | 1466 | $\delta(H^{12}\text{-}C^{7}\text{-}H^{11})$ 86% |
| 15 | 1427 | 1431 | $\delta(H^{13}\text{-}N^{4}\text{-}H^{17})$36% + $\tau(H^{11}\text{-}C^{7}\text{-}C^{9}\text{-}N^{5})$ 22% |
| 16 | 1404 | 1421 | $\delta(H^{13}\text{-}N^{4}\text{-}H^{17}$42% - $\tau(H^{11}\text{-}C^{7}\text{-}C^{9}\text{-}N)$ 20% |
| 17 | 1363 | 1385 | $\nu_{sym}(O^{2}=C^{8}=O^{1})$ 10% + $\tau(H^{10}\text{-}C^{6}\text{-}C^{8}=O^{1})$ 47% |
| 18 | | 1354 | $\nu_{sym}(O^{2}=C^{8}=O^{1})$ 34% –$\tau(H^{10}\text{-}C^{6}\text{-}C^{8}\text{-}O^{1})$ 17% |
| 19 | | 1331 | $\nu(N^{5}\text{-}C^{9})$ 10% + $\nu_{sym}(O^{2}=C^{8}=O^{1})$ 15%+ $\delta(H^{10}\text{-}C^{6}\text{-}C^{7})$ 34% |
| 20 | 1300 | 1307 | $\nu_{sym}(O^{2}=C^{8}=O^{1})$ 15% + $\delta(H^{11}\text{-}C^{7}\text{-}C^{9})$ 12% –$\nu(N^{5}\text{-}C^{9})$ 17% |
| 21 | 1237 | 1228 | $\delta(H^{11}\text{-}C^{7}\text{-}C^{9})$ 39% |
| 22 | 1144 | 1167 | $\nu(C^{7}\text{-}C^{6})$ 21%+ $\delta(H^{10}\text{-}C^{6}\text{-}C^{7})$ 19% + $\tau(H^{13}\text{-}N^{4}\text{-}C^{6}\text{-}C^{7})$ 19% |
| 23 | 1102 | 1106 | $\delta(H^{15}\text{-}N^{5}\text{-}C^{9})$ 30% + $\tau(H^{13}\text{-}N^{4}\text{-}C^{6}\text{-}C^{7})$ 14% |
| 24 | 1075 | 1084 | $\nu(N^{5}\text{-}C^{9})$ 11%+ $\delta(H^{15}\text{-}N^{5}\text{-}C^{9})$ 21% – $\tau(H^{13}\text{-}N^{4}\text{-}C^{6}\text{-}C^{7})$ 28% |
| 25 | 1005 | 1050 | $\nu(C^{7}\text{-}C^{6})$ 15%– $\nu(N^{4}\text{-}C^{6})$ 27% –$\tau(H^{13}\text{-}N^{4}\text{-}C^{6}\text{-}C^{7})$ (14) |
| 26 | | 970 | $\nu(C^{7}\text{-}C^{6})$ 20% –$\tau(H^{13}\text{-}N^{4}\text{-}C^{6}\text{-}C^{7})$ 18% –$\tau(H^{12}\text{-}C^{7}\text{-}C^{9}\text{-}N^{5})$ 10% |
| 27 | 912 | 934 | $\nu(N^{4}\text{-}C^{6})$ 34% – $\tau(H^{13}\text{-}N^{4}\text{-}C^{6}\text{-}C^{7})$ 11% + $\tau(H^{12}\text{-}C^{7}\text{-}C^{9}\text{-}N^{5})$ 14% |
| 28 | 888 | 874 | $\nu(C^{9}\text{-}C^{7})$ 54% |
| 29 | 838 | 839 | $\nu(O^{1}=C^{8})$ 11%+ $\nu(C^{8}\text{-}C^{6})$ 29% + $\delta(O^{2}\text{-}C^{8}\text{-}O^{1})$ 35% |
| 30 | 799 | 759 | $\delta(O^{2}=C^{8}=O^{1})$ 14%+ $\gamma(O^{2}=C^{6}=O^{1}\text{-}C^{8})$ 44% |
| 31 | 662 | 697 | $\gamma(O^{3}=C^{7}\text{-}N^{5}\text{-}C^{9})$ 48% |
| 32 | 603 | 623 | $\delta(C^{8}\text{-}C^{6}\text{-}N^{4})$ 10% –$\delta(C^{6}\text{-}C^{8}=O^{1})$ 15% –$\tau(H^{15}\text{-}N^{5}\text{-}C^{9}\text{-}C^{7})$ 38% |
| 33 | 567 | 596 | $\nu(C^{8}\text{-}C^{6})$ 11% + $\delta(C^{6}\text{-}C^{8}\text{-}O^{1})$ 49% |
| 34 | 521 | 527 | $\tau(H^{15}\text{-}N^{5}\text{-}C^{9}\text{-}C^{7})$ 40% –$\delta(C^{6}\text{-}C^{8}\text{-}O^{1})$ 15% |
| 35 | | 511 | $\nu(C^{8}\text{-}C^{6})$ 20%– $\delta(O^{2}=C^{8}=O^{1})$ 15% – $\delta(C^{6}=C^{8}=O^{1})$ 11% – $\tau(H^{15}\text{-}N^{5}\text{-}C^{9}\text{-}C^{7})$ 13% |
| 36 | 412 | 432 | $\delta(N^{5}\text{-}C^{9}\text{-}C^{7})$ 64% |
| 37 | | 346 | $\delta(C^{6}\text{-}C^{8}=O^{1})$ 21%+ $\delta(C^{8}\text{-}C^{6}\text{-}N^{4})$ 16% + $\gamma(C^{8}\text{-}N^{4}\text{-}C^{7}\text{-}C^{6})$ 22% |
| 38 | | 329 | $\delta(C^{7}\text{-}C^{6}\text{-}N^{7})$ 53% |
| 39 | | 296 | $\tau(H^{15}\text{-}N^{5}\text{-}C^{9}\text{-}C^{7})$ 92% |
| 40 | | 270 | $\tau(H^{13}\text{-}N^{4}\text{-}C^{6}\text{-}C^{7})$ 74% |
| 41 | | 259 | $\delta(C^{6}\text{-}C^{8}=O^{1})$ 14% + $\delta(C^{8}\text{-}C^{6}\text{-}N^{4})$ 21% – $\gamma(C^{8}\text{-}N^{4}\text{-}C^{7}\text{-}C^{6})$ 24% |
| 42 | | 163 | $\delta(C^{6}\text{-}C^{7}\text{-}C^{9})$ 69% |
| 43 | | 76 | $\tau(C^{9}\text{-}C^{7}\text{-}C^{6}\text{-}N^{4})$ 76% |
| 44 | | 70 | $\tau(C^{6}\text{-}C^{7}\text{-}C^{9}\text{-}N^{5})$ 67% |
| 45 | | 49 | $\tau(N^{4}\text{-}C^{6}\text{-}C^{8}=O^{1})$ 65% |

* ν – stretching, δ – bending, τ – torsion, γ – out-of-plane vibration, sym – symmetric, asym – asymmetric.

©Academy of Sciences of Republic of Uzbekistan, 2023

## IV. Conclusion

In this work, the structural, electronic, and vibrational physical-chemical properties of zwitterionic L-asparagine were investigated using Raman spectroscopy and the density functional theory (DFT) method. Also, molecular geometry, vibrational spectra, electron density distribution in atoms, the molecular electrostatic potential (MEP) of surface, frontier molecular orbitals (FMO), atoms in molecules (AIM), non-covalent interaction (NCI), reduced density gradient (RDG), and analysis such as electronic localization function (ELF) were performed. The molecular geometry of ZWASN was optimized using the 6-311++G(d,p) basis in the B3LYP approximation. The calculated geometric parameters (bond length and angle) were compared with the experimental results and found to be in good agreement. For the first time, the charge distribution in atoms was calculated. Topological analyses confirmed the presence of N-H···O internal H-bonds in the ZWASN molecule. Using FMO analysis, parameters of ZWASN such as the HOMO-LUMO energy gap, ionization energy, chemical potential, hardness, electron affinity, and global electrophilicity index were determined for the first time. The theoretically calculated and experimentally observed wave numbers were compared and found to be in good agreement. These experimental and computational results will help in studying the physical-chemical properties of L-asparagine.

## References


[1] P.T. Reidy, B.B. Rasmussen. J. Nutr. **146**, 155-183 (2016). https://doi.org/10.3945/jn.114.203208.

[2] T. Pazderka, V. Kopecký Jr. Spectrochim. Acta A: Mol. Biomol. Spectrosc. **185**, 207-216 (2017). https://doi.org/10.1016/j.saa.2017.05.043.

[3] A. Marcu, A. Stanila, O. Cozar, L. David. J. Optoelect. Adv. Mater. **10**, 830-833 (2008).

[4] S.S. Patil, G.A. Thakur, M.M. Shaikh. ISRN Pharm. **6**, 168539 (2011). https://doi.org/10.5402/2011/168539

[5] L.F. Krylova, L.M. Kovtunova, G.V. Romanenko, L.A. Sheludyakova. J. Struct. Chem. **51**, 1152-1163 (2010).

[6] E. Lim, S. Park, J. Byun, C.-S. Hwang.Nanocrystals. Bull. Korean Chem. Soc. **33**, 1741-1747 (2012).

[7] S. Gronert, R.A.J. O'Hair. Amer. Chem. Soc. **117**, No.7, 2071-2081 (1995). https://doi.org/10.1021/ja00112a022

[8] Y.C. Tse, M.D. Newton, S. Vishveshwara, J.A. Pople. J. Amer. Chem. Soc. **100**, 4329 (1978). https://doi.org/10.1021/ja00482a001

[9] S.G. Stepanian, I.D. Reva, E.D. Radchenko, L. Adamowicz. J. Phys. Chem. A **103**, No.22, 4404-4412 (1999). https://doi.org/10.1021/jp984457v

[10] Shahrzad Shirazian, Scott Gronert. J. Mol. Struct. **397**, 107-112 (1997). https://doi.org/10.1016/S0166-1280(96)04939-1

[11] M.M. Ali Gina, M. Umadevi, B. Ravikumar, V. Ramakrishnan. Spectrochim. Acta A: Mol. Biomol. Spectrosc. **60**, No.13, 2977-2983 (2004). https://doi.org/10.1016/j.saa.2004.02.010

[12] A. Jumabaev, U. Holikulov, H. Hushvaktov, A. Absanov, L. Bulavin. Ukr. J. Phys. **67**, No.8, 602-610 (2022). https://doi.org/10.15407/ujpe67.8.602

[13] P. Skurski, M. Gutowski, R. Barrios, J. Simons. Chem. Phys. Lett. **337**, 143-150 (2001). https://doi.org/10.1016/S0009-2614(01)00166-X

[14] G. Nandini, D.N. Sathyanarayana. J. Phys. Chem. A **107**, 51, 11391-11400 (2003). https://doi.org/10.1021/jp030979l

[15] M. Shakir, S.K. Kushawaha, K.K. Maurya, S. Kumar, M.A. Wahab, and G. Bhagavannarayana. J. Appl. Cryst. **43**, 491-497 (2010). https://doi.org/10.1107/S0021889810008745P.

[16] C. Aleman, J. Puiggali. J. Phys. Chem. B **101**, 3441-3446 (1997). https://doi.org/10.1021/jp963425

[17] B. Imperiali, K.L. Shannon, K.W. Rickert. J. Amer. Chem. Soc. **114**, 7942–7944 (1992). https://doi.org/10.1021/ja00046a068

[18] B. Li, R.T. Borchardt, E.M. Topp, D. Vander Velde, R.L. Schowen. J. Amer. Chem. Soc. **125**, 11486-11487 (2003). https://doi.org/10.1021/ja0360992

[19] S.E. O'Connor, B. Imperiali. J. Amer. Chem. Soc. **119**, 2295-2296 (1997). https://doi.org/10.1021/ja963435o

[20] J.L. Radkiewicz, H. Zipse, S. Clarke, K.N. Houk. J. Amer. Chem. Soc. **118**, 9148-9155 (1996). https://doi.org/10.1021/ja953505b

[21] M.L. Chen, Z.J. Huang, Z.J. Lin. J. Mol. Struct. **719**, 153-158 (2005). https://doi.org/10.1016/j.theochem.2005.01.019

[22] T. Kimura, N. Matubayasi, H. Sato, F. Hirata, M. Nakahara. J. Phys. Chem. B **106**, 12336-12343 (2002). https://doi.org/10.1021/jp021246o

[23] J. Casado, F.J. Ramirez, J.T.L. Navarrete. J. Mol. Struct. **349**, 57-60 (1995). https://doi.org/10.1016/0022-2860(95)08708-4

[24] M.J. Frisch, G.W. Trucks, H.B. Schlegel, G.E. Scuseria, M.A. Robb, J.R. Cheeseman, G. Scalmani, V. Barone, B. Mennucci, G.A. Petersson, H. Nakatsuji, M. Caricato, X. Li, H.P. Hratchian, A.F. Izmaylov, J. Bloino, G. Zheng, J.L. Sonnenberg, M. Hada, M. Ehara, K. Toyota, R. Fukuda, J. Hasegawa, M. Ishida, T. Nakajima, Y. Honda, O. Kitao, H. Nakai, T. Vreven, J.A. Montgomery, Jr., J.E. Peralta, F. Ogliaro, M. Bearpark, J.J. Heyd, E. Brothers, K.N. Kudin, V.N. Staroverov, R. Kobayashi, J. Normand, K. Raghavachari, A. Rendell, J.C. Burant, S.S. Iyengar, J. Tomasi, M. Cossi, N. Rega, J.M. Millam, M. Klene, J.E. Knox, J.B. Cross, V. Bakken, C. Adamo, J. Jaramillo, R. Gomperts, R.E. Stratmann, O. Yazyev, A.J. Austin, R. Cammi, C. Pomelli, J.W. Ochterski, R.L. Martin, K. Morokuma, V.G. Zakrzewski, G.A. Voth, P. Salvador, J.J. Dannenberg, S. Dapprich, A.D. Daniels, Ö. Farkas, J.B. Foresman, J.V. Ortiz, J. Cioslowski, and D.J. Fox. Gaussian 09 (Gaussian, Inc., Wallingford CT, 2009).

[25] M.Kh. Khodiev, U.A. Holikulov, N. Issaoui, O.M. Al-Dossary, L.G. Bousiakoug, N.L. Lavrik. J. King Saud Univ.


©Academy of Sciences of Republic of Uzbekistan, 2023

Sci. **35**, No.3, 102530 (2023). https://doi.org/10.1016/j.jksus.2022.102530
[26] T. Lu, F. Chen. J. Comput. Chem. **33**, 580–592 (2012). https://doi.org/10.1002/jcc.22885
[27] W. Humphrey, A. Dalke, K. Schulten. J. Mol. Graph. **14**, No.1, 33-38 (1996). https://doi.org/10.1016/0263-7855(96)00018-5
[28] K. Yamada, D. Hashizume, T. Shimizu, and S. Yokoyama. Acta Cryst. E **63**, 3802-3803 (2007). https://doi.org/10.1107/S1600536807039505
[29] T. Koopmans. Physica **1**, 104-113 (1934). https://doi.org/10.1016/S0031-8914(34)90011-2
[30] T.-H. Tang, E. Deretey, S.J. Knak Jensen, and I.G. Csizmadia. Eur. Phys. J. D **37**, 217-222 (2006). https://doi.org/10.1140/epjd/e2005-00317-0
[31] M.H. Jamroz. Spectrochim. Acta A Mol. Biomol. Spectrosc. **114**, 220-230 (2013).

## L-аспарагиннинг структуравий, электрон ва тебраниш хусусиятлари

**Ў.А. Холикулов**

Самарқанд давлат университети, Университет хиёбони 15, 140104, Самарқанд, Ўзбекистон

Ушбу ишда L-аспарагиннинг структуравий, электрон ва тебраниш хусусиятлари Раман спектроскопияси ва зичлик функционал назарияси (DFT) ҳисоблашлари ёрдамида ўрганилган. L-аспарагиннинг цвиттер-ион тузилишининг молекуляр геометрияси B3LYP/6-311++G(d,p) базислар тўплами асосида оптималлаштирилди. Цвиттерион L-аспарагиндаги (ZWASN) ички H-боғланиш молекуляр электростатик потенциал (MEP) сирти, молекуладаги атомлар (AIM), қисқартирилган зичлик градиенти (RDG), ноковалент таъсир (NCI) ва электрон локализация функцияси (ELF) усуллари ёрдамида таҳлил қилинди. Шунингдек, Малликен атом заряд тақсимоти, HOMO-LUMO энергия фарқи ва бошқа электрон хусусиятлари ҳисобланди. Экспериментал Раман спектри қайд қилинди ва PED усули ёрдамида таҳлил қилинди.

**Калит сўзлар:** L-аспарагин, цвиттер-ион, H-боғланиш, Раман спектроскопияси, DFT методи.

©Academy of Sciences of Republic of Uzbekistan, 2023